A.A. ZAREMBA, P.Yu. ZAREMBA, F.V. MUCHNYK, H.V. BARANOVA, S.D. ZAHORODNIA*

D.K. Zabolotny Institute of Microbiology and Virology, NAS of Ukraine,
154 Akademika Zabolotnoho Str., Kyiv, 03143, Ukraine
* Author for correspondence; e-mail: svetazagorodnya@ukr.net

IN SILICO IDENTIFICATION OF A VIRAL SURFACE GLYCOPROTE IN SITE SUITABLE FOR THE DEVELOPMENT OF LOW MOLECULAR MASS INHIBITORS FOR VARIOUS VARIANTS OF SARS-COV-2

Severe acute respiratory syndrome-related coronavirus 2 (SARS-CoV-2) is a new coronavirus today has an extremely significant impact on both the global economy and society as a whole, due to its pandemic status and risk of complications. Therefore, understanding the molecular features of the interaction of receptor binding domain (RBD), which determines most of the dangerous properties of this pathogen, with human angiotensin-converting enzyme 2 (hACE2) is an important step in the process of developing a successful strategy to combat SARS-CoV-2. In addition, given the significant rate of accumulation of mutations in RBD, it makes sense to consider its different variants. **Goal.** *Identification of a pocket potentially suitable for the search for low molecular mass inhibitors of the interaction of different variants of SARS-CoV-2 RBD and hACE2.* **Methods.** *The initial structure of different variants of the RBD/hACE2 complex was obtained from Protein Data Bank (PDB). Separate RBD variants were isolated from the same data. To obtain the Y453F mutant, variant P.1 was mutagenized in PyMol 1.8. The construction of the system, which included the resulting associate or individual protein, solvent, and physiological concentration of sodium chloride, was performed using CHARMM-GUI (graphical user interface for CHARMM) tools according to the standard protocol for glycoproteins. The actual simulation and balancing of the system were performed in GROMACS (GROningen MAchine for Chemical Simulation) version 2019.6 for 50 ns.* **Results.** *The interface of the RBD/hACE2 interaction is formed by amino acids Q24, D30, H34, E35, E37, Y41, Y83, K353, D355, and R393 for hACE2 and K417, Y453, F486, N487, Y489, Q493, Q498, T500, N501, and Y505 — for RBD. However, it is heterogeneous and can be divided into two subinterfaces, and each either of them includes its own pool of interactions: hACE2 Q24/Y83 + RBD N487, hACE2 H34 + RBD Y453, hACE2 E35 + + RBD Q493, and hACE2 D30 + RBD K417 for N- terminal relative to H1 hACE2 subinterface and hACE2 E37/R393 + + RBD Y505, hACE2 K353 + RBD Q498/G502, and hACE2 D355 + RBD T500 — for C-terminal. According to the considered N501Y mutation, changes are observed in the mentioned interaction patterns — hydrogen bonds of hACE2*

A.A. Zaremba, P.Yu. Zaremba, F.V. Muchnyk, H.V. Baranova, S. D. Zahorodnia

Q42 + RBD Q498, hACE2 K31 + RBD Q493, and hACE2 K31 + RBD F490 are formed, and hACE2 H34 + RBD Y453 is lost. Similar aberrations, except for the hydrogen bond with F490, are observed in the case of the N501Y + Y453F variant. Despite significant changes in the pool of interactions, the gross number of hydrogen bonds for the complexes of all three variants is relatively stable and ranges from 9 to 10. The defined interaction for all considered variants of RBD are characterized by the presence of a pocket between the subinterfaces, which is formed by the residues R403, Y453, Q493, S494, Y495, G496, F497, Q498, N501, and Y505 conditionally original variant. According to the results of the molecular dynamics simulation, the Y453F replacement has little effect on the overall topology of the cavity but sufficiently reduces the polarity of the pocket part of its localization, which leads to the impossibility of forming any polar interactions. In contrast, N501Y, due to a larger size of the tyrosine radical and the presence of parahydroxyl, forms two equivalent mutually exclusive hydrogen bonds with the carbonyls of the peptide groups G496 and Y495. Additional stabilization of Y501 is provided by interplanar stacking with Y505. In addition to the anchored position in ~ 25% of the trajectory, there is another "open" conformation Y501, at which the radical of this tyrosine does not interact with the rest of the protein. **Conclusions.** 1) The interface of the interaction of SARS-CoV-2 RBD with hACE2 is not continuous, and it can be conditionally divided into two subinterfaces: N-terminal and C-terminal. Either of them is characterized by its own pattern of connections and changes according to the RBD N501Y and Y453F replacements considered. However, despite the presence of significant molecular rearrangements caused by N501Y and Y453F, the total number of hydrogen bonds is almost the same for all mutants. 2) Between the identified interaction subinterfaces, SARS-CoV-2 RBD contains a caveola, which due to its location may be potentially suitable for finding promising candidates for drugs aimed at inhibiting the interaction of this protein with hACE2. In this case, the replacements of N501Y and Y453F have a significant impact on the topology of a particular pocket and can potentially modify the activity of inhibitors directed to this area.

Keywords: SARS-CoV-2, receptor binding domain (RBD), mutation N501Y, mutation Y453F, human angiotensin-converting enzyme 2 (hACE2), GROMACS, CHARMM-GUI.

Severe acute respiratory syndrome-related coronavirus 2 (SARS-CoV-2) is a new coronavirus that is believed to start in late 2019 in Wuhan (the People's Republic of China) [1]. The virus spread rapidly around the world, and on March 11, 2020, the World Health Organization (WHO) officially declared a pandemic. In November of 2021, the number of reported cases of COVID-19 exceeded 261 million (of which 5.2 million people died) worldwide [2]. Just for comparison, the SARS-CoV virus in 2002—2003 infected about 8,500 people in 27 countries and caused 866 deaths [3].

S-glycoprotein (spike) is a major factor influencing the properties of this virus, such as high contagion, host specificity, and tropism. It ensures the attachment of the virion to the permissive target cell with the subsequent fusion of the viral and host membranes. The latter is mediated by membrane-anchored human angiotensin-converting enzyme 2 (hACE2), which hydrolyzes the S-glycoprotein into two daughter proteins S1 and S2, which in turn allows the fusion peptide to interact with the cell membrane and leads to the release of the virion nucleocapsid into the cytosol. The initiation of these molecular processes is provided by a small receptor-binding domain (RBD) present in the apical region of the S-glycoprotein. It is its potent interaction with hACE2 that is the main trigger for the virus to enter the cell.

Also, the recent tendencies of SARS-CoV-2 to actively counteract human immunity and vaccination, which are manifested in the accumulation of both conditionally neutral and potentially dangerous mutations in all parts of its genome, should be taken into account. Of particular note are the replacements in the S-glycoprotein and, in fact, RBD, because they can not only help this virus to counteract the immune defense of the microorganism but also, due to the lability of the structure, greatly complicate the potential development of low molecular mass drugs aimed at this protein [4].

Thus, the **aim** of our work is to identify a pocket potentially suitable for the search for

low molecular mass inhibitors of the interaction of different variants of SARS-CoV-2 RBD and hACE2.

Materials and Methods. The initial structure of different variants of the RBD/hACE2 complex was obtained from RCSB PDB (PDB ID: 6M0J and 7NXC) [5]. The initial preparation of the associates was performed using PyMol 1.8 [6] and included the removal of crystalline water, ions, and small organic molecules. Additionally, in the same program, the P.1 variant (7NXC) was modified to simulate the replacement of tyrosine for phenylalanine at position 453 of the RBD. The system was built using CHARMM-GUI tools [7] according to the standard protocol for glycoproteins (force field CHARMM36m) and involved the creation of a cubic box with periodic boundary conditions, which contained glycoprotein complex RBD/hACE2, water as a solvent (model TIP3P), as well as Na⁺ and Cl⁻ ions of physiological concentration (0.15 M). Typical for these protein disulfide bonds were also reproduced. The system temperature was 303.15 K. Equilibration and molecular modeling (50ns) were performed in GROMACS 2019.6 [8] using GPU as an accelerator. The trajectory analysis was performed using PyMol 1.8 software and built-in GROMACS utilities.

Results. *Analysis of the molecular dynamics of different variants of RBD in combination with hACE2.* Basing on the trajectory of simulation of molecular dynamics of the complex of **non-mutant** RBD with hACE2, we can identify amino acid residues that, by forming stable hydrogen bonds, are directly involved in their interaction: Q24, D30, H34, E35, E37, Y41, Y83, K353, D355 and R393 for hACE2 and K417, Y453, F486, N487, Y489, Q493, Q498, T500, N501, and Y505 — for RBD (Fig. 1). Thus, a sufficiently long interface of the topological correspondence of the S1 receptor-recognizing domain to hACE2 is formed.

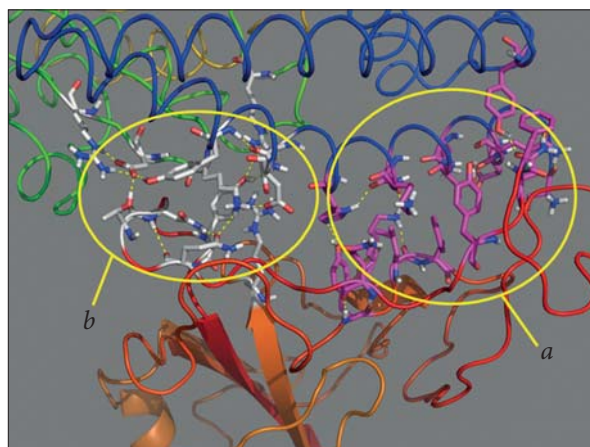The interaction of RBD with hACE2 is not homogeneous. Within one large interface de-

Fig. 1. The area of interaction of non-mutant RBD with hACE2: *a* — the first interaction subinterface; *b* — the second interaction subinterface
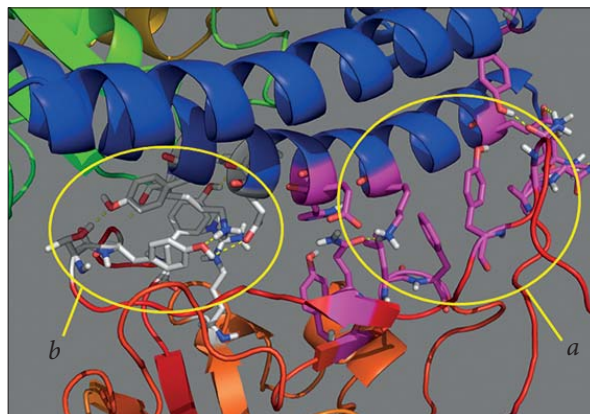

Fig. 2. RBD interaction site with replacement of N501Y with hACE2: *a* — the first interaction subinterface; *b* — the second interaction subinterface

scribed above, two subinterfaces can be clearly distinguished as follows.

1. The first one covers the N-terminus of H1 hACE2 (tyrosine-83 is part of H2) and the corresponding part of RBD (Fig. 1, A). The main stabilizing interactions here are the hydrogen bonds hACE2 Q24/Y83 + RBD N487, hACE2 H34 + RBD Y453, and hACE2 E35 + RBD Q493, as well as the ionic bond hACE2 D30 + RBD K417. Additional stabilization is provided by RBD F486, which shields the hydrogen bond of hACE2 Y83 + RBD N487 from the effects of the
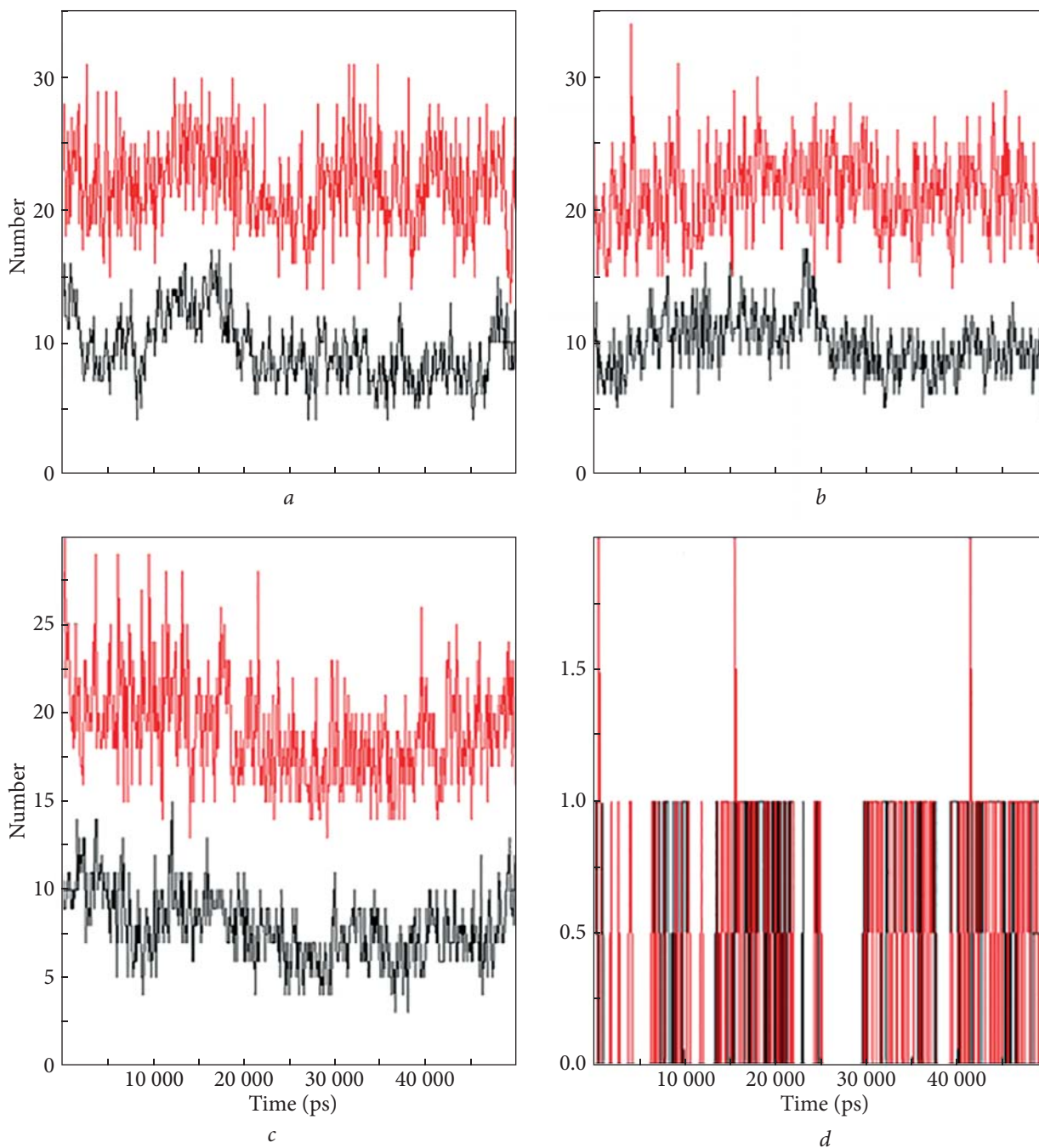
Fig. 3. Dependence of the number of formed hydrogen bonds on the simulation time: *a* — between the wild variant of RBD and hACE2; *b* — between the N501Y variant of RBD and hACE2; *c* — between the N501Y + Y453F variant of RBD and hACE2; *d* — between RBD 501 and carbonyl G496/Y495

solvent and forms an interplanar stacking with the same amino acids.

2. The second one is located at the C-terminus relative to H1 hACE2 (amino acids K353, D355, and R393 are part of the central beta-folded structure) and covers the corresponding part of the RBD (Fig. 1, B). The main guiding interactions here are the hydrogen bonds of hACE2 E37/R393 + RBD Y505, hACE2 K353 + RBD Q498/G502, and hACE2 D355 + RBD T500. Interestingly, the hydrogen bond of hACE2 K353 + RBD G502 is observed not between the radical of one of them (K353) and the peptide group of the other, but between their peptide groups (carbonyl K353 and amide G502), which may indicate the high stability of the position of the parts of the proteins in which they are relative to each other.

The molecular dynamics of the N501Y mutant in complex with hACE2 differs from that described above in for the replacement of asparagine by tyrosine (Fig. 2). The amino acid hACE2 K353, along with the preserved bond with RBD G502, loses interaction with RBD Q498. Tyrosine 501 recruits Q498 by forming an intrachain hydrogen bond. In parallel, the amide of this glutamine forms a stable hydrogen bond with hACE2 Q42, thus, acting as a mediator. Additionally, the stabilization of Y501 is provided by forming a T-shaped stacking of Y41. In the central part of the interaction site, the RBD amino acid Q493, which previously formed only one hydrogen bond with hACE2 E35, interacts with hACE2 K31 as well, which further fixes its position. The more ordered lysine radical 31 also forms a stable, non-mutant RBD-specific bond with F490 carbonyl. In contrast, the interaction of hACE2 H34 with RBD Y453 was manifested only in T-stacking, without the formation of a hydrogen bond. The remaining interactions of the N501Y RBD/hACE2 complex were similar to those for non-mutant RBD.

A similar situation, with some changes, is observed in the case of N501Y + Y453F. Due to the replacement of tyrosine with phenylalanine at position 453, any orienting interactions could not be formed in this area. In addition, the above-mentioned additional hydrogen bond hACE2 K31 + RBD F490, characteristic of the N501Y mutant, was ~~also~~ not observed in this case either.

The dynamics of the total number of hydrogen bonds formed by the considered variants of RBD indicates the relative stability of their gross quantity over the course of the simulation (Fig. 3). In all three cases, their number ranged from 9 to 10. However, the overall level of interactions between RBD and hACE2, as indicated by the dynamics of paired contacts (~ 3.5 A), is slightly higher for the complex of non-mutant S1 receptor-recognizing domain. The N501Y mutant is characterized by greater stability of this pool of interactions.

Analysis of topological features of different RBD variants in the area of interaction with hACE2. The surface of all RBD variants in the area of contact with hACE2 is very similar and (what is important for us) is characterized by a pronounced cavern between the defined by us subinterfaces of interaction (Fig. 4). It is formed by residues R403, Y453, Q493, S494, Y495, G496, F497, Q498, N501, and Y505 of the conditionally initial variant (Fig. 4, B). Accordingly, variants with N501Y and Y453F replacements at these positions have other amino acids. It just so happened that these mutations are at opposite ends of our pocket (Fig. 4, A). Y453F has little effect on the overall topology of this area, but the lack of a highly polar hydroxyl group makes this part of the pocket much more hydrophobic and, as a result, incapable of forming hydrogen bonds.

In contrast, N501Y is not so synonymous. Due to a larger size of the radical and the presence of parahydroxyl, this amino acid forms two equivalent hydrogen bonds with the carbonyls of peptide groups G496 and Y495, which fixes its position and partially covers the selected pocket (Fig. 5, B). Additional stabilization of Y501
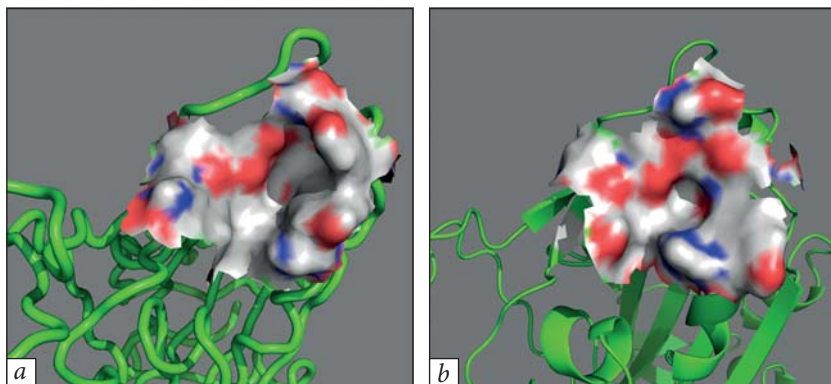
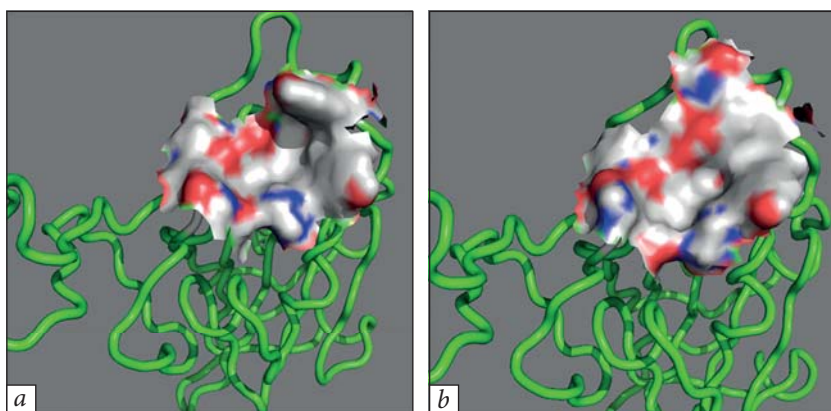Fig. 4. RBD pocket: *a* — mutant N501Y + Y453F; *b* — unchanged RBD

Fig. 5. RBD N501Y pocket: *a* — a disordered form of Y501; *b* — a fixed form of Y501

is provided by interplanar stacking with Y505. However, this amino acid may be in another form, not fixed by hydrogen bonds (Fig. 5, A).

In this case, its radical is in direct contact with the solvent and does not form ordered interactions with the rest of the RBD. The ratio of these two forms in our simulation was ~ 3:1 (Fig. 3, D).

Discussion. A large amount of data is now available on both specific RBD and S-glycoprotein in general [9—11]. Many studies have already tried to determine the potentially most suitable pocket or pockets for interaction with a potential drug [12—14]. In most of them, after identification of the most acceptable binding site (s), virtual screening of substance libraries was performed to identify potentially effective SARS-CoV-2 inhibitors. However, all of these studies target only the original S1 receptor-binding do-

main, which can potentially lead to the lack of activity of discovered compounds against new variants of SARS-CoV-2, similar by etiology to what we see today in the case of currently available vaccines [15, 16]. Instead, in our work, we consider several variants of SARS-CoV-2 RBD, one original and two mutants.

The molecular dynamics of the considered RBDs, despite the replacement, was generally similar: the gross number of hydrogen bonds and the total number of paired contacts fluctuated similarly for all variants. Only some greater stability and number of interactions of 0.35 nm, which was observed during the simulation of molecular dynamics of non-mutant RBD, can, with some probability, indicate its greater potential for the formation of a complex with hACE2. Nevertheless, a thorough analysis of the molecular dynamics trajectory of all three variants sug-

gests significant changes in the configuration of the RBD/hACE2 interaction interface.

In particular, the replacement of N501Y made it impossible to form the hydrogen bond hACE2 K353 + RBD Q498. In this case, the vacant amino acid Q498 stably interacts as a hydrogen bond donor with hydroxyl tyrosine 501 and as an acceptor/donor with hACE2 Q42. Thus, in the case of the mentioned replacement, one more hydrogen bond is formed in the region of the selected C-terminal subinterface of the interaction. In addition, tyrosine, compared to asparagine, contains a much larger conjugate electron cloud. Therefore, the T-shaped stacking of Y41 will also affect the stability of the complex of the considered variant with hACE2. Also, along with the formation of additional interactions between hACE2 K31 and RBD Q493/F490, the contact of hACE2 H34 with RBD Y453 is lost, which also adds one theoretical hydrogen bond.

The molecular dynamics of the complex variant N501Y + Y453F in general was very similar to that for N501Y. However, additional replacement of tyrosine with phenylalanine at position 453 led to an increase in the hydrophobicity of this area. Moreover, the absence of hydroxyl in the para-position reduced the size of the radical itself, which potentiated the hACE2 H34 to the formation of interplanar stacking with RBD Q493. This, in turn, stabilized the hydrogen bonds of Q493 with hACE2 K31/E35 and reduced the likelihood of lysine 31 interacting with RBD F490.

Thus, if we take into account the general similarity of the dynamics of the number of hydrogen bonds in all three cases and the mentioned changes in the interaction site, we can assume that, despite induction by the considered replacements of rather significant rearrangements of patterns of communications between RBD and hACE2, the total affinity of the S1 receptor-binding domain for its target is approximately the same as in the original variant.

Therefore, fundamentally, despite the findings of some researchers [17, 18], who link the replacements of N501Y and Y453F with a direct increase in the affinity of SARS-CoV-2 RBD to hACE2, we consider these mutations as a consequence of evolutionary pressure unrelated to the RBD/hACE2 complex formation efficiency. It is likely that the evolutionary gains that accompany such changes are associated with an increased likelihood of avoiding the neutralizing effects of antibodies present in convalescents or vaccinated individuals. This is supported by significant molecular rearrangements in the region of interaction of RBD with hACE2 (especially for our selected C-terminal subinterface), which can be evolutionarily selected so as to weakly affect the efficiency of key processes in the life cycle of SARS-CoV-2 and, at the same time, to allow this virus to avoid the suppressive effect on the human immune system to some extent [19].

Identification of potentially acceptable for interaction with low molecular mass **cavern** on the surface of a key protein (in this case, a domain), and RBD is undoubtedly such [20], is one of the necessary steps in the search/development of target drugs.

Direct competitive blocking is one of the most promising and time-tested ways to inhibit receptor-ligand interactions. Therefore, the pocket between the RBD/hACE2 interaction subinterfaces described above is, in our opinion, a promising candidate for the development of a competitive inhibitor of the first stages of the SARS-CoV-2 life cycle. It should be noted that we are not the first to pay attention specifically to this part of the protein [21]. The replacements considered by us are located directly in the identified pocket and can strongly modify its topological features. Thus, N501Y reduces the linear size of the caveola. Tyrosine in this position forms two stable mutually exclusive hydrogen bonds with G496 and Y495, which strongly stabilizes its position and potentially prevents the interaction of the drug candidate with RBD in this area. However,

over the course of modeling, we found a rarer conformation of this amino acid. In about 25% of the simulations, the tyrosine 501 residue did not form any orienting interactions with the rest of the protein, thus opening about 20% of the pockets for a potential inhibitor. Therefore, it can be argued that in the case of finding candidates for drugs directed to this site, it makes sense to use at least two conformations of RBD as a receptor.

Replacement of Y453F did not affect the pocket topology so much. Tyrosine and phenylalanine are similar in their characteristics to amino acids. However, the absence of para-hydroxyl, as we have already mentioned, reduced the polarity of the corresponding part of the cavity and, as a consequence, led to the impossibility of forming orientational interactions. Thus, a compound that is potentially active against the wild-type RBD variant, which is also focused on the formation of hydrogen bonds in this region, can change its activity quite strongly in the case of the Y453F variant, which should also be considered at the earliest possible stages of drug development.

In summary, it can be argued that in the case of SARS-CoV-2 and specifically RBD, an effective search for potential targeted drugs should include both classical identification of a suitable cavity and changes in the pocket of the virus population. *Because*, as we have mentioned, replacements in the selected area can greatly mod-ify its topology, which in the long run, at later stages of development, can result in significant losses of both material and mental resources.

Conclusions

1. By analyzing the simulation of molecular dynamics, it was determined that the interface of the interaction of SARS-CoV-2 RBD with hACE2 is not continuous and can be divided into two subinterfaces: N-terminal and C-terminal. Either of them is characterized by its own pattern of connections and changes according to the RBD N501Y and Y453F replacements considered. However, despite the presence of significant molecular rearrangements caused by N501Y and Y453F, the total number of hydrogen bonds is almost the same for all mutants.

2. Between the SARS-CoV-2 interaction subinterfaces identified by us, RBD contains a caveola, which due to its location may be potentially suitable for finding promising candidates for drugs aimed at inhibiting the interaction of this protein with hACE2. In this case, the replacements of N501Y and Y453F have a significant impact on the topology of a particular pocket and can potentially modify the activity of inhibitors directed to this area.

Thus, the identified pocket is potentially suitable for the search for low molecular mass inhibitors of the interaction *of different variants of SARS-CoV-2 RBD and hACE2* and will allow targeted docking for the development of promising antiviral compounds.

REFERENCES

1. Syed A, Khan A, Gosai F, Asif A, Dhillon S. Gastrointestinal pathophysiology of SARS-CoV2 — a literature review. Journal of community hospital internal medicine perspectives. 2020; 10(6):523—28.
2. Dong E, Du H, Gardner L. An interactive web-based dashboard to track COVID-19 in real time. Lancet Infect Dis. 2020; 20(5):533—34.
3. Chan-Yeung M, Xu RH. SARS: epidemiology. Respirology. 2003; 8(1):9—14.
4. Sanyaolu A, Okorie C, Marinkovic A, Haider N, Abbasi AF, Jaferi U, Prakash S, Balendra V. The emerging SARS-CoV-2 variants of concern. Ther Adv Infect Dis. 2021; 8:20499361211024372.
5. Berman HM, Westbrook J, Feng Z, Gilliland G, Bhat TN, Weissig H, Shindyalov IN, Bourne PE. The Protein Data Bank. Nucleic Acids Research. 2000; 28:235—42.
6. The PyMOL (1.7.4.4 Edu) Molecular Graphics System, Version 1.8 Schrödinger, LLC. Available at: http://www.pymol.org/pymol.

7. Lee J, Cheng X, Swails JM, Yeom MS, Eastman PK, Lemkul JA, et al. CHARMM-GUI Input Generator for NAMD, GROMACS, AMBER, OpenMM, and CHARMM/OpenMM Simulations using the CHARMM36 Additive Force Field. J Chem Theory Comput. 2016; 12:405—13.

8. Abraham MJ, Murtola T, Schulz R, Páll S, Smith JC, Hess B, Lindahl E. GROMACS: High performance molecular simulations through multi-level parallelism from laptops to supercomputers. SoftwareX. 2015; 1—2:19—25.

9. Duan L, Zheng Q, Zhang H, Niu Y, Lou Y, Wang H. The SARS-CoV-2 Spike Glycoprotein Biosynthesis, Structure, Function, and Antigenicity: Implications for the Design of Spike-Based Vaccine Immunogens. Front Immunol. 2020; 11:576622.

10. Ou X, Liu Y, Lei X, Li P, Mi D, Ren L, Guo L, Guo R, Chen T, Hu J, Xiang Z, Mu Z, Chen X, Chen J, Hu K, Jin Q, Wang J, Qian Z. Characterization of spike glycoprotein of SARS-CoV-2 on virus entry and its immune cross-reactivity with SARS-CoV. Nat Commun. 2020; 11(1):1620.

11. Walls AC, Park YJ, Tortorici MA, Wall A, McGuire AT, Veesler D. Structure, Function, and Antigenicity of the SARS-CoV-2 Spike Glycoprotein. Cell. 2020; 181(2):281—92.

12. Behloul N, Baha S, Guo Y, Yang Z, Shi R, Meng J. In silico identification of strong binders of the SARS-CoV-2 receptor-binding domain. Eur J Pharmacol. 2021; 890:173701.

13. Gervasoni S, Vistoli G, Talarico C, Manelfi C, Beccari AR, Studer G, Tauriello G, Waterhouse AM, Schwede T, Pedretti AA. Comprehensive Mapping of the Druggable Cavities within the SARS-CoV-2 Therapeutically Relevant Proteins by Combining Pocket and Docking Searches as Implemented in Pockets 2.0. Int J Mol Sci. 2020; 21(14):5152.

14. Feng S, Luan X, Wang Y, Wang H, Zhang Z, Wang Y, Tian Z, Liu M, Xiao Y, Zhao Y, Zhou R, Zhang S. Eltrombopag is a potential target for drug intervention in SARS-CoV-2 spike protein. Infect Genet Evol. 2020; 85:104419.

15. Hacisuleyman E, Hale C, Saito Y, Blachere NE, Bergh M, Conlon EG, Schaefer-Babajew DJ, DaSilva J, Muecksch F, Gaebler C, Lifton R, Nussenzweig MC, Hatziioannou T, Bieniasz PD, Darnell RB. Vaccine Breakthrough Infections with SARS-CoV-2 Variants. N Engl J Med. 2021; 384(23):2212—18.

16. Planas D, Veyer D, Baidaliuk A, Staropoli I, Guivel-Benhassine F, Rajah MM, Planchais C, Porrot F, Robillard N, Puech J, Prot M, Gallais F, Gantner P, Velay A, Le Guen J, Kassis-Chikhani N, Edriss D, Belec L, Seve A, Courtellemont L, Péré H, Hocqueloux L, Fafi-Kremer S, Prazuck T, Mouquet H, Bruel T, Simon-Lorière E, Rey FA, Schwartz O. Reduced sensitivity of SARS-CoV-2 variant Delta to antibody neutralization. Nature. 2021; 596(7871):276—80.

17. Williams AH, Zhan CG. Fast Prediction of Binding Affinities of the SARS-CoV-2 Spike Protein Mutant N501Y (UK Variant) with ACE2 and Miniprotein Drug Candidates. J Phys Chem B. 2021; 125(17):4330—36.

18. Aljindan RY, Al-Subaie AM, Al-Ohali AI, Kumar DT, Doss CGP, Kamaraj B. Investigation of nonsynonymous mutations in the spike protein of SARS-CoV-2 and its interaction with the ACE2 receptor by molecular docking and MM/GBSA approach. Comput Biol Med. 2021; 135:104654.

19. Supasa P, Zhou D, Dejnirattisai W, Liu C, Mentzer AJ, Ginn HM, Zhao Y, Duyvesteyn HME, Nutalai R, et al. Reduced neutralization of SARS-CoV-2 B.1.1.7 variant by convalescent and vaccine sera. Cell. 2021; 184(8):2201—11.

20. Hoffmann M, Kleine-Weber H, Schroeder S, Krüger N, Herrler T, Erichsen S, Schiergens TS, Herrler G, Wu NH, Nitsche A, Müller MA, Drosten C, Pöhlmann S. SARS-CoV-2 Cell Entry Depends on ACE2 and TMPRSS2 and Is Blocked by a Clinically Proven Protease Inhibitor. Cell. 2020; 181(2):271—80.

21. Trezza A, Iovinelli D, Santucci A, Prischi F, Spiga O. An integrated Miniprotein Drug Candidates. J Phys Chem B. 2021; 125(17):4330—36.

А.А. Заремба, П.Ю. Заремба, Ф.В. Мучник, Г.В. Баранова, С.Д. Загородня

Інститут мікробіології і вірусології ім. Д.К. Заболотного НАН України,
вул. Академіка Заболотного, 154, Київ, 03143, Україна

IN SILICO ІДЕНТИФІКАЦІЯ ДІЛЯНКИ ВІРУСНОГО ПОВЕРХНЕВОГО ГЛІКОПРОТЕЇНУ, ПРИДАТНОЇ ДЛЯ РОЗРОБКИ НИЗЬКОМОЛЕКУЛЯРНИХ ІНГІБІТОРІВ РІЗНИХ ВАРІАНТІВ SARS-COV-2

Severe acute respiratory syndrome-related coronavirus 2 (SARS-CoV-2) є новим коронавірусом, який нині, через свій пандемічний статус та небезпеку ускладнень, чинить надзвичайно значний вплив на загальносвітову економіку та суспільство. S-глікопротеїн (Spike), а саме його рецептор-зв'язуючий домен (RBD), є основною структурно-функціональною одиницею даного вірусу, яка визначає специфічність SARS-CoV-2 до поверхневих білків клітин людського організму. Тому розуміння молекулярних особливостей взаємодії RBD з ангіотензинперетворюючим ферментом 2 людини (hACE2) є важливим кроком процесу розробки успішної стратегії боротьби з даним патогеном. Крім того, беручи до уваги значну швидкість накопичення мутацій в RBD, є сенс враховувати і різні його варіанти. **Мета**. Ідентифікація кишені, потенційно придатної для пошуку низькомолекулярних інгібіторів взаємодії RBD різних варіантів SARS-CoV-2 та hACE2. **Методи**. Вихідна структура різних варіантів комплексу RBD/hACE2 була отримана з Protein Data Bank (PDB). Окремо варіанти RBD були виділені з цих же даних. Для отримання мутанта Y453F варіанта P.1 був використаний функціонал PyMol 1.8. Побудова системи, яка включала отриманий асоціат або ж окремий білок, розчинник та фізіологічну концентрацію натрій хлориду проводилась інструментарієм CHARMM-GUI (graphical user interface for CHARMM) за стандартним протоколом для глікопротеїнів та включала генерацію всіх вихідних дисульфідних зв'язків. Власне моделювання та врівноваження системи виконувалися в GROMACS (GROningen MAchine for Chemical Simulation) версії 2019.6 протягом 50 наносекунд (нс). **Результати**. Інтерфейс взаємодії RBD з hACE2 формується амінокислотами Q24, D30, H34, E35, E37, Y41, Y83, K353, D355 і R393 — для hACE2 та K417, Y453, F486, N487, Y489, Q493, Q498, T500, N501 і Y505 — для RBD. При цьому він є неоднорідним і його умовно можна поділити на два субінтерфейси, кожен з яких включає свій пул взаємодій: hACE2 Q24/Y83 + RBD N487, hACE2 H34 + RBD Y453, hACE2 E35 + RBD Q493 і hACE2 D30 + RBD K417 — для N-кінцевого відносно H1 hACE2 субінтерфейсу та hACE2 E37/R393 + RBD Y505, hACE2 K353 + RBD Q498/G502 і hACE2 D355 + RBD T500 — для С-кінцевого. Відповідно до розглянутої мутації N501Y спостерігаються зміни в згаданих паттернах взаємодій — формуються водневі зв'язки hACE2 Q42 + RBD Q498, hACE2 K31 + RBD Q493 та hACE2 K31 + RBD F490 і втрачається зв'язок hACE2 H34 + RBD Y453. Схожі аберації спостерігаються й у випадку варіанта N501Y + Y453F. Додатково відзначається відсутність водневого зв'язку hACE2 K31 + RBD F490. Попри достатньо значні зміни пулу сформованих взаємодій, загальна кількість водневих зв'язків для комплексів всіх трьох варіантів є відносно стабільною та коливається в межах 9—10. Між визначеними субінтерфейсами взаємодії для всіх розглянутих варіантів RBD є характерною наявність кишені, яка формується залишками R403, Y453, Q493, S494, Y495, G496, F497, Q498, N501 та Y505 вихідного варіанту. За результатами симуляції молекулярної динаміки, заміна Y453F слабо впливає на загальну топологію каверни, однак достатньо знижує полярність частини кишені своєї локалізації, що призводить до неможливості формування будь-яких полярних взаємодій. Натомість N501Y через більший розмір радикалу тирозину та наявність парагідроксилу формує два рівнозначних взаємовиключних водневих зв'язки з карбонілами пептидних груп G496 та Y495. Додаткова стабілізація Y501 забезпечується міжплощинним стекінгом з Y505. Окрім заякореного положення в ~25 % траєкторії, зустрічається й інша «відкрита» конформація Y501, за якої радикал даного тирозину не взаємодіє з рештою білка. **Висновки.** 1) Інтерфейс взаємодії SARS-CoV-2 RBD з hACE2 не є суцільним, і його умовно можна поділити на два субінтерфейси: N-кінцевий та С-кінцевий, кожен з яких характеризується своїм паттерном сформованих зв'язків та змінюється відповідно до розглянутих нами амінокислотних замін RBD N501Y та Y453F. Однак, попри наявність значних молекулярних перебудов, спричинених N501Y та Y453F, загальна кількість водневих зв'язків є відносно однаковою для всіх мутантів. 2) Між ідентифікованими субінтерфейсами взаємодії SARS-CoV-2 RBD містить кавеолу, яка завдяки своєму розташуванню може бути потенційно придатною для пошуку перспективних структур та розробки на її основі ліків, направлених на інгібування взаємодії даного білка з hACE2. При цьому заміни N501Y та Y453F чинять достатньо значний вплив на топологію визначеної кишені та потенційно можуть модифікувати активність інгібіторів, направлених на цю ділянку.

Ключові слова: SARS-CoV-2, рецептор-зв'язуючий домен (RBD), мутація N501Y, мутація Y453F, людський ангіотензин-перетворюючий фермент 2 (hACE2), GROMACS, CHARMM-GUI.